International Journal of Steel Structures
June 2014, Vol 14, No 2, 421-438
DOI 10.1007/s13296-014-2020-2

International Journal of
STEEL
STRUCTURES
www.springer.com/journal/13296

A Review on Assessment of Fatigue Strength in Welded Studs

Jörg Hildebrand[1] and Hadi Soltanzadeh[2,*]

[1]*Prof. Dr.-Ing., Bauhaus-Universität Weimar, Fakultät Bauingenieurwesen, Simulation und Experiment, Marienstraße 7A, 99421 Weimar, Germany*
[2]*Ph.D. Student in Bauhaus-Universität Weimar, Fakultät Bauingenieurwesen, Simulation und Experiment, Marienstraße 7A, 99421 Weimar, Germany*

Abstract

Welding is one of the most important and highly developed joining methods; nevertheless unwanted side effects occur like thermal strains and altering of certain material properties induced by heating and melting. These effects lead to distortions and high residual stresses which should be kept to a minimum. To minimize distortion, various strategies are being developed. Stud welding is widely used in steel structures, power plants, and ship buildings due to the significantly technology including highest quality of production processes by continuous electrical control and the efficiency of such a process. Therefore, varying the heat input typically will affect the material properties including yield strength, tensile strength, hardness, and notch toughness in the stud arc welding. Well-defined heat sources offer a reproduced heat input into a highly localized area. The fatigue strength of stud welding has been investigated by performing welding process and microstructural observations. This paper is going to discuss the influence of heat input on the structural changes in stud arc welding.

Keywords: stud welding process, material strength, hardening behavior, fatigue strength

1. Introduction

Radaj (1990) considered that the arc pressure welded joint between the stud and base plate is mainly used in structural steel engineering (head stud in steel-concrete composite girders) as well as in shipbuilding (Eyres and Bruce, 2012), pipe (NS Stud Welding Method, 2013), tank (Tank Car Committee, 2013), and boiler construction (Roberts and Dogan, 1998). Special applications of stud welding could include the construction of facades and vehicles (Jenicek *et al*., 2006), on wear resistant surfacing (Clegg *et al*., 1983), steel stud on aluminum plates (Ramasamy, 2000), underwater stud welding (Masubuchi *et al*., 1978).

The principles of stud welding are adopted from arc welding. Arc welding is a very complicated phenomenon, which, in particular includes heat transfer, mass transfer, metallurgical reaction, element diffusion, microstructure change, and variation of mechanical properties (Dean *et al*., 2007). Arc stud welding is a highly reliable fastening method for a wide variety of applications. The process can quickly weld almost any size or configuration of metal stud to a workpiece, with maximum weld penetration and reliability. Figure 1 shows the types and principle applications of the stud welding processes. Stud welding is roughly classified into arc stud welding and capacitor discharge (CD) stud welding.

According to (Behrens *et al*., 2011) the capacitor discharge method is limited to studs of 8 mm and less for economic reasons. In addition to this, low insertion of energy and only needed one-sided accessibility are other restrictions for this type of welding. Because of these limitations, this process is used less than with the arc welding process for heavy fabrication.

It is worth pointed out that for application where strength is not the primary requirement, the parent metal thickness may be reduced (CD process specification) whilst in this research it was focused only on drawn arc stud welding process since this type of welding is very often used in many productions. The stud arc welding process includes the same electrical, thermal, metallurgical, and mechanical principles as other arc welding processes. The welding parameters (current and arc time) depend on the material type and size of the stud base (Hamza, 2012). Li *et al*. (2003) observed in order to carry out the welding simulation work precisely; the combination of thermal

Note.-Discussion open until November 1, 2014. This manuscript for this paper was submitted for review and possible publication on October 29, 2013; approved on April 14, 2014.

*Corresponding author
Tel: +49-3643-584442; Fax: +49-3643-584441
E-mail: hadi.soltanzadeh@uni-weimar.de

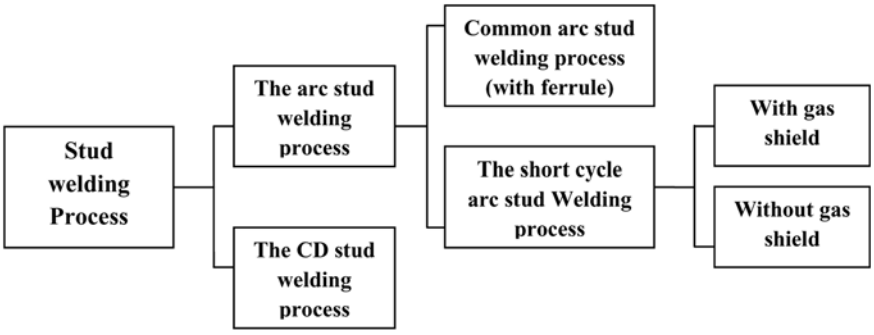

Figure 1. The types of the stud welding processes (Nishikawa, 2003).

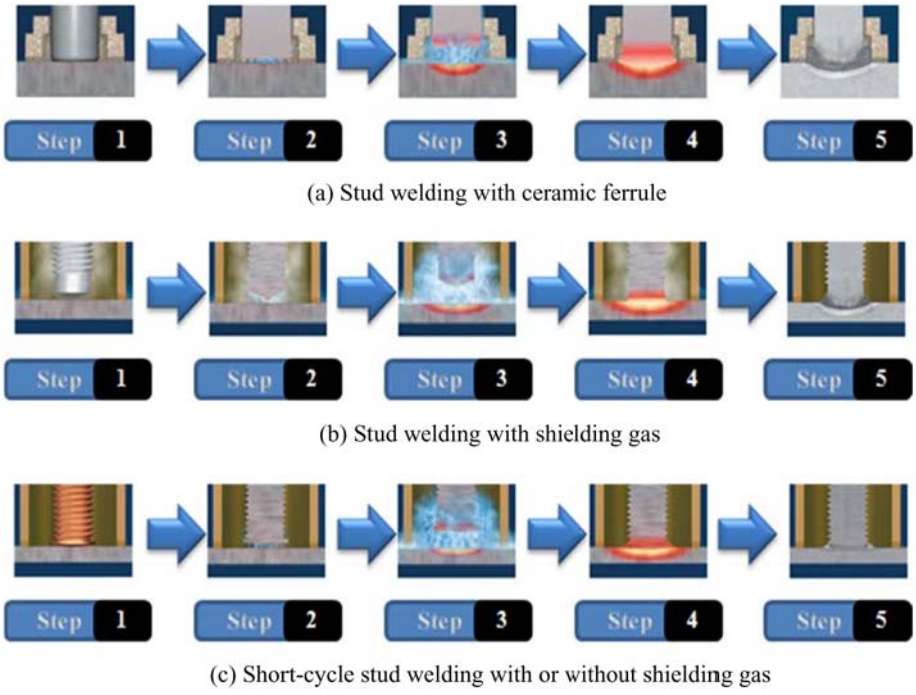

Figure 2. Drawn arc stud welding processes (Köster Co., 2013).

and mechanical properties during welding for stud welding is the main issue.

2. Specific of Stud Welding

With respect to the Fig. 2 and Table 1, there are three common techniques of arc stud welding: drawn arc stud welding, short arc stud welding and gas arc stud welding.

As explained, depending on the application, drawn arc stud welding is available with the following variants (Köster Co.):

(1) In the drawn arc technique, the stud is loaded into the chuck of the welding gun, and a ferrule (a disposable ceramic shield that contains the molten pool of metal) is placed over the end. The gun is placed against the workpiece. When the trigger is pressed, the DC power supply sends a signal that energizes the gun's internal lift mechanism, lifting the stud and drawing the pilot arc. The pilot arc establishes a path for the weld current, which initiates after the pilot arc. Upon completion of the correct arcing time, which is proportional to the square area of the surface being melted, the lift mechanism is de-energized. This causes the stud to plunge into the molten pool of metal. Typical length reductions of studs in Arc Stud Welding are illustrated in Table 2. A plunge dampener is often used on larger studs to decelerate the stud's movement

Table 1. Illustration of steps for drawn arc stud welding (Köster Co., 2013)

Step 1	The stud is placed against the workpiece
Step 2	The stud is lifted off while current is flowing, thus creating an arc
Step 3	The arc melts the surface of the stud and work-piece
Step 4	The stud is plunged into the weld pool
Step 5	A cross-sectional joint is achieved

Table 2. Typical length reduction of studs in arc stud welding (Köster Co.)

Stud Diameters	Length Reductions
3/16 through 1/2 in. (4.8 through 12.7 mm)	1/8 in. (3.2 mm)
5/8 through 7/8 in. (4.8 through 12.7 mm)	3/16 in. (4.8 mm)
1 in. and over (25.4 mm and over)	3/16 to 1/4 in. (4.8 to 6.4 mm)

onto the molten pool. This minimizes splash. As the stud and the base metal join, the metal begins to solidify and the weld is created. The gun is lifted, and the ferrule is discarded.

(2) The gas arc technique uses inert shielding gas with no flux or ferrule, making it easier to automate. However, it provides less fillet control and less penetration depth compared with the drawn arc technique. In gas arc welding, a spark shield, which delivers the gas, replaces the ferrule. The stud is loaded and the gun is positioned for welding. When the user pulls the trigger, shielding gas floods the welding zone. The stud is lifted, and an arc is generated. While the stud remains lifted, the weld current melts the stud and base metal. When the arc time is complete, the stud is plunged into the molten pool. More gas is blown onto the weld, flowing until the molten metal cools. The gun can then be removed. Because no ferrule is used, this process lends itself well to automation and robotics.

(3) The short arc technique is much like drawn arc, except that it uses no flux load or ferrule. This technique offers the shortest welding times of the arc stud welding techniques. It is characterized by high currents and short weld times. While it may be suitable for many high-volume applications, it can produce porous welds and should therefore be selected when speed and cost are a priority over weld strength for an investigation into the possible causes of the undesirable variability in the stud welding process, the researcher modifies a cause-and-effect diagram that lists several suspected causes of this variability; the Fig. 3 illustrates the cause and effect of the problem being studies (Hamza, 2012). According to Samardzic *et al*. (2009), quality concerns traditionally associated with drawn arc welding process are related to variables inherent in stud welding (weld current, weld time, arc voltage, plunge, depth, etc.) and more general manufacturing variables (cleanliness, joint geometry, etc.). Some of the factors that cause weld stud failures are incorrect base plate material or plate surface condition, inappropriate weld settings and lack of quality control. It illustrates that the stud welding process are divided into four main groups:

1. the stud sheet group. The factors that can be affected this group are:

• sheet material

• sheet thickness: It has little or no effect on metallurgical weld quality. Increasing sheet thickness has two effects. First, a thicker sheet is stiffer during mechanical testing. Also, thicker steels present a greater cross section to tearing, creating inherently stronger welds. As a result, stiffness of the joint is only slightly affected by sheet thickness, with subsequently little impact on torsion strength performance (AWS).

• sheet coating: Internal porosity in the joint is not as big a factor for shear tests and presence of the coating not as big a concern (AWS).

• sheet preheating

2. The stud group

• stud design: Larger studs are going to have a greater bonding area and subsequently greater strength. Also, larger studs have substantially greater torsional rigidity and, thus, dominate in the torque tests (AWS).

• stud material: According to chamber's studies (2001) studs of all styles are available in low carbon steel and various grades of stainless steel.

• stud diameters

3. The setup welding operations group: In respect to chamber's investigation (2001) in the basic process, DC (direct current) power from a self-contained generator or transformer/rectifier is passed through a stud welding

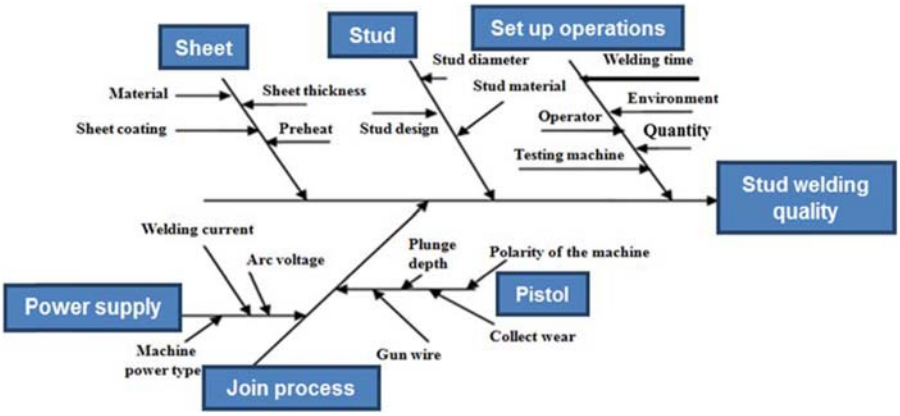

Figure 3. The suggested stud welding cause and effect diagram (Hamza, 2012).

control system. The control system is set at a determined time, voltage, and amperage to initiate the arc, which forms the molten pool.

- the welding time adjustment
- the quantity of studs to be welded
- the operator performance
- the environment

4. The joint process

This item is being mentioned into two parts:

- The power supply properties (voltage, current, machine power type (Continuous Electric Arc or Direct Capacitor Arc))
- The pistol properties (gun wear (new or old), the polarity of the machine, the plunge depth and the gun wire

In respect to the above mentioned the following figure illustrates the cause and effect of such these problems which can be encountered during process.

For the full strength of the stud, the base metal thickness should be at least 1/3 of the stud base diameter. Sheet material has a large effect on the tensile strength standard deviation, while the stud material has a smaller effect (Hamza, 2012).

3. Electric Effect on the Welding Process

The field properties around welding equipment are primarily defined by the properties of the welding current, which is dependent on the welding process and the capabilities of the power-source used (Mair, 2005). The importance of amperage on welding quality with weld defects resulting from welding current variation can be affected (Al-Sahib *et al*., 2009). During the welding cycle, Al-Sahib *et al*. (2009) also presented a relationship between the stud lift, arc voltage and current generated by the welding power supply. Several steps of the stud movement relative to the surface are illustrated in Fig. 4.

As Fig. 4 illustrates for arc stud welding with tip ignition the lift height, which determines the arc length, is the distance the gun will raise the stud above the welding surface during the weld. This distance governs the voltage and the arc. Improper lift will cause unsatisfactory welds. The current path sharp angle represents that there exits the electrode (stud) and enters the workpiece.

Beside that Behrens *et al*. (2011) shown as depicted in Figure 5, the automated welding process is controlled by current flow and arc voltage as well as the movement of the stud.

As shown in Fig. 5 the role of amperage is best understood in the context of heat input. Amperage is a measure of the amount of current flowing through the electrode and the work. One way to determine arc voltage is to measure the voltage drop between the contact surface and workpiece (for instance here is 1.5 ms). Rocha *et al*. (2012) also carried out a study on the effect of the cross-section area of the stud shanks and the steel

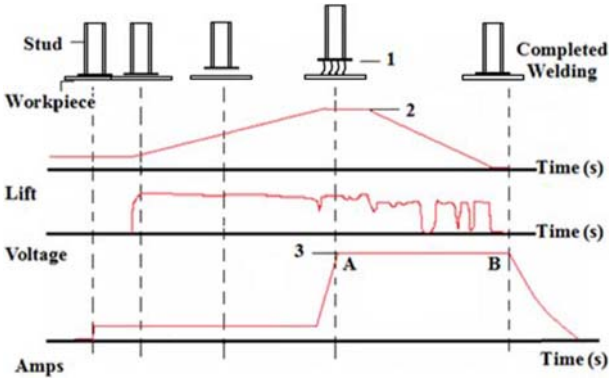

Figure 4. Stud movement relative to the surface during welding (Al-Sahib *et al*., 2009). 1. Maximum intensive electric arc, 2. Maximum stud lift, 3. Current peak value.

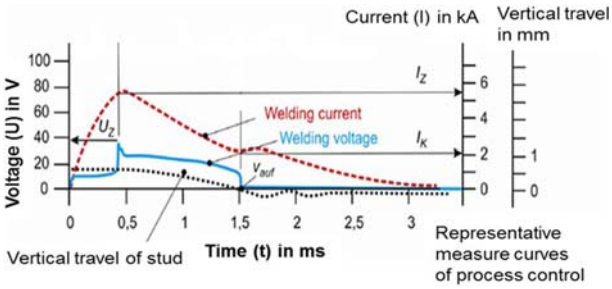

Figure 5. Illustration depicting the electric effect on the welding process (Gruβ, 2013).

Table 3. Representation of standard studs (Taylor Co.)

Stud type	Actual diameter (mm)	Weld current (A)	Weld time (ms)
5FB	5	400	100
6RB	4.7	376	94
6FB	6	480	120
8RB	6.2	496	124
8FB	8	640	160
10RB	7.9	632	158
10FB	10	800	200
12RB	9.5	760	190
12FB	12	960	240
16RB	13.2	1058	528

FB: full based diameter, RB: reduced based diameter

strength on the stud strength by using numerical simulation. Accordingly (Hsu *et al*., 2007), one challenge in stud welder design is the ability to quickly react to arc conditions and input power fluctuations since the total arc time is typically 25-35 ms. (Taylor Co.) A set of basic formulae as defined (Table 2) by the British Standard BS EN ISO 14555:2006 Annex A.2.7.2.2 and Annex 2.7.2.4 may be used to calculate the current and time settings to weld any stud. These formulae, when applied to standard studs, give the results shown in the Table 3.

4. Metallurgical Considerations and Melting-solidification Behavior

The metallurgical structures encountered arc stud welds are generally the same as those found in any arc weld where the heat of an electric arc is used to melt both a portion of the base metal and the electrode (stud) in the course of welding. Acceptable mechanical properties are obtained when the stud and base material are metallurgically compatible (Kuehn *et al*., 1997). To make a good weld occur, two things are needed: heat and pressure. Lack of one or the other affects weld quality. Sufficient heat must be there to melt the weld zone, and if there is not enough pressure there, good fusion will not occur (International Welding Technologies Inc., 2003). It should be mentioned that the more pressure the weld has, the shorter the weld time will be. This will result in a cooler weld with less penetration (International welding technologies, 2003). David *et al*. (2003) indicated that an important aspect of weld solidification is the dynamic of weld pool development. Thermal conditions in and near the weld pool and the nature of the fluid flow have been found to influence the size and shape of the weld pool. GSI SLV München (2011) observed that depending on the weld pool which has a different weld shape during immersion of displaced melt generated around the bolt, the choice of ceramic rings and shielding gases may be different. Depending on the weld pool, which has a different weld shape during immersion of displaced melt generated around the bolt, it was also observed that the choice of ceramic rings and shielding gases may be different.

As the severity of thermal excursions experienced by the material varies from region to region in the weldment, (David *et al*., 2003) thus the growth rate and temperature gradient differ considerably across the weld pool (GSI SLV München, 2011). Li *et al*. (2003) generalized that the quantitative explanation of the solidification process has been improved by thermal transmission mass transfer and the kinetics of moving interface. To understand the effects of microstructure on the mechanical performance of welds, it is important to recognize microstructural differences at the various weld regions. These include the base metal (BM), heat affected zone (HAZ) and fusion zone (FZ). The FZ is created by heating above the melting point, while the surrounding HAZ material itself consists of several regions which experience thermal cycles with progressively decreasing peak temperature from the fusion boundary (Khan *et al*., 2008).

4.1. Effect of process parameters on HAZ

To distinguish the metallurgy of the welded joint, it has been taken into account Dong *et al*. (2013) studies. They categorized the metallurgy of the friction stir weld joint (Fig. 6) into: The natural level Nugget zone (NZ), experiences the highest peak temperature as well as an intense plastic deformation and the hardness of the NZ which depends on the different welding speeds. The thermo-mechanically affected zone (TMAZ) is characterized by elongated grains with a high density of dislocations. The welding speed did not have a significant effect on hardness in this zone. The HAZ is located between the TMAZ and the BM (Base Metal), and experiences only the thermal cycle, not deformation. The peak temperature in the HAZ close to the TMAZ is much higher than the peak temperature close to the BM. The hardness of the TMAZ is lower than that of the NZ but higher than the HAZ. Compared with the HAZ, the hardness increase in the TMAZ can be explained by the density of dislocations which were induced by the plastic deformation during welding. The effect of temperature susceptibility on the microstructure in the weld area has serious influence which tends to change in a great manner the microstructure conditions in the fusion zone and in the HAZ.

Bhadeshia and Honeycombe (2006) concluded that the HAZ, on the other hand, represents those regions in the close proximity of the weld where the heat input during welding changes the microstructure without melting the steel. However, the region of the metal being welded is small compared to the remaining mass of steel plate. The plate forms a heat sink and hence the metal in the region of the weld is cooled fairly rapidly. The existence of large areas of unheated metal adjoining the HAZ in fact form a heat sink and the HAZ is cooled more rapidly than the as-rolled plate when it is initially air cooled after rolling. It is possible that the grain size had grown so large and the cooling time had become shortened enough to prevent

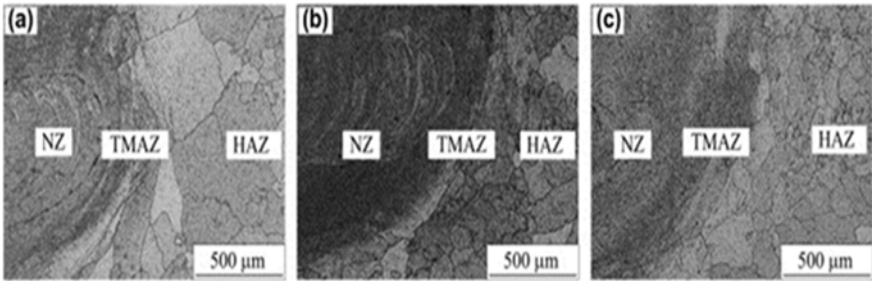

Figure 6. Optical microstructures of the TMAZ and the HAZ at the welding speeds of 100 mm min^{-1} (a), 200 mm min^{-1} (b) and 400 mm min^{-1} (c) (Dong *et al*., 2013).

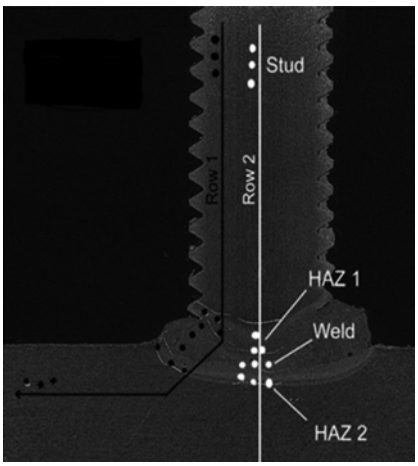

Figure 7. Macro-cut and hardness rows for a stud-weld with M8 studs (Row 1 along the edge and row 2 in center) (Fricke and Tchuindjang, 2012).

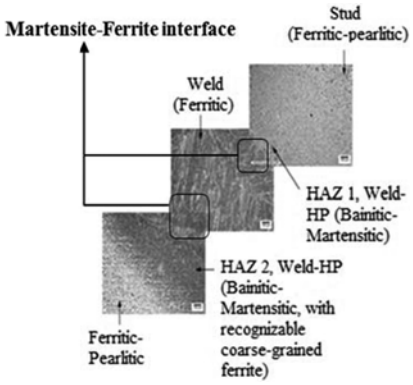

Figure 8. Micro-structure of a stud-weld (Fricke and Tchuindjang, 2012).

normal precipitation of the ferrite at the grain boundaries (Williams *et al*., 1970). Based on Fricke and Tchuindjang (2012) investigation the hardness measurements were performed for two rows per specimens (Fig. 7) according to Vickers HV5. The highest values occur in the weld and in the heat-affected zone (HAZ 2), as shown in Fig. 7 between weld and parent metal. The parent metal of profile shows a ferritic-pearlitic structure with recognizable lines due to rolling (Fricke and Tchuindjang, 2012). Only by improving the microstructure of the HAZ can the properties of a welded joint be improved (Srivastava *et al*., 2010). According to Calcagnotto *et al*. (2011) and with respect to Fig. 8 chiefly, mechanical properties deformation and fracture mechanisms can be studied based on microstructure observations using scanning electron microscopy (SEM). Moreover, the stress/strain partitioning characteristics between ferrite and martensite change due to grain refinement, leading to enhanced martensite plasticity and better interface cohesion.

The microstructures developed in the weld metal and heat-affected zone (HAZ) of a fusion welding process

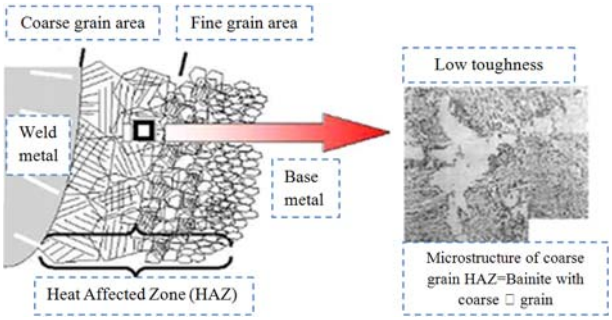

Figure 9. Problem in HAZ of high heat input welded joint (Kitani *et al*., 2007).

play an important role in controlling the mechanical properties of weldments (Joarder *et al*., 1991).

4.2. Improvement of HAZ toughness for high Heat Input welding

4.2.1. Effect of arc energy

According to Hsu and Mumaw reaserch (2011), arc energy has a direct impact on the weld strength and visual defects. Too little energy results in insufficient fusion and thus compromises weld strength; too much energy results in dimple and melt-through. The heat necessary for welding of studs is developed from a DC power source between the stud and workpiece to which the stud is to be welded. Welding time and the plunging of the stud into the molten weld pool to complete the weld are controlled automatically through the power source. Because stud arc welding time cycles are very short, heat input to the base metal is very small compared to conventional arc welding. Consequently, the weld metal and heat-affected zones are very narrow and distortion of the base metal at stud locations is minimal. In terms of high heat input welding as depicted in Fig. 9, HAZ toughness is deteriorated where it can have important and detrimental effects on the microstructure and equally on the mechanical properties of the material constituting the heat affected zone (Ambriz and Mayagoitia, 2011). By increasing heat input austenite grain growth in the HAZ becomes remarkable and the coarse-grain austenite region expands (Kitani *et al*., 2007) because the coarse-grain microstructure consisting of ferrite side plates at prior austenite grain boundaries and intra-granular upper bainite has low toughness, HAZ toughness is greatly reduced.

5. Stress State during and after the Stud Welding Process

Many researchers (Dai, 2012) have noted that chemical composition and condition of welding materials can directly affect fatigue crack growth rates of welded joints. Therefore phase change will occur in most kinds of steel when subjected to the welding process and residual stresses are introduced by these phase changes. It is worth noting that

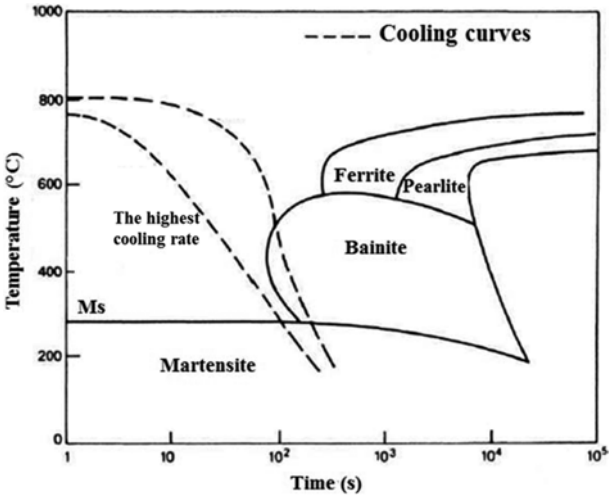

Figure 10. Typical CCT diagram for steel (Bhadeshia and Honeycombe, 2006).

the importance of having accurate information in relation to the transformation temperatures of steels for residual stress during welding process (Dai *et al*. 2008). Such information is usually presented in the form of CCT diagrams (Fig. 10). They are plotted for the onset and completion of reactions to form pearlite, bainite and martensite. Depending on diversity cooling conditions different microstructures can be derived.

As it has been already mentioned by Elmer *et al*. (1982) it is evident that changes in composition result in formation of phases with different thermal expansion properties. Peet *et al*. (2011) have reported that thermal conductivity controls the magnitude of the temperature gradients which occur in components during manufacture and use. A suitable model of thermal conductivity should help to improve the design of steels and understanding of heat treatment, solidification, welding processes and prediction of thermo-mechanical fatigue. In reality the thermal conductivity will depend upon the microstructure of the steel.

Table 4. The chemical composition of S355

Grade S355 / Yield strength	C%	Si%	Mn%	Cr%	Ni%	Mo%
355 N/mm^2	0.162	0.282	1.508	0.013	0.013	0.005

The Fig. 11 is largely based on numerical data obtained using a modern calculation software like SYSWELD made from special grades of steel (S355). Table 4 shows the chemical composition of S355.

In practice, metallurgical phase diagrams are usually represented in terms of weight percentages. In each cooling rate, the number of phases, their properties and their percentages are represented.

When the HAZ is rapidly quenched, the austenite cannot transform into the more stable ferrite phase because the carbon atoms mechanically hinder the rearrangement of the iron atoms into a ferrite phase and martensite. Cho and Kim (2002) conclude that metallurgical phase transformation must be considered in welding residual stress analysis especially for medium and high carbon steel. Figure 12 depicts thermal conductivity for different phases versus temperature. A great deal of so-called force can be produced at around 700°C by preventing the deformed martensite to austenite. The melting point and boiling point for austenite will be around 1,500 and 2,500°C respectively.

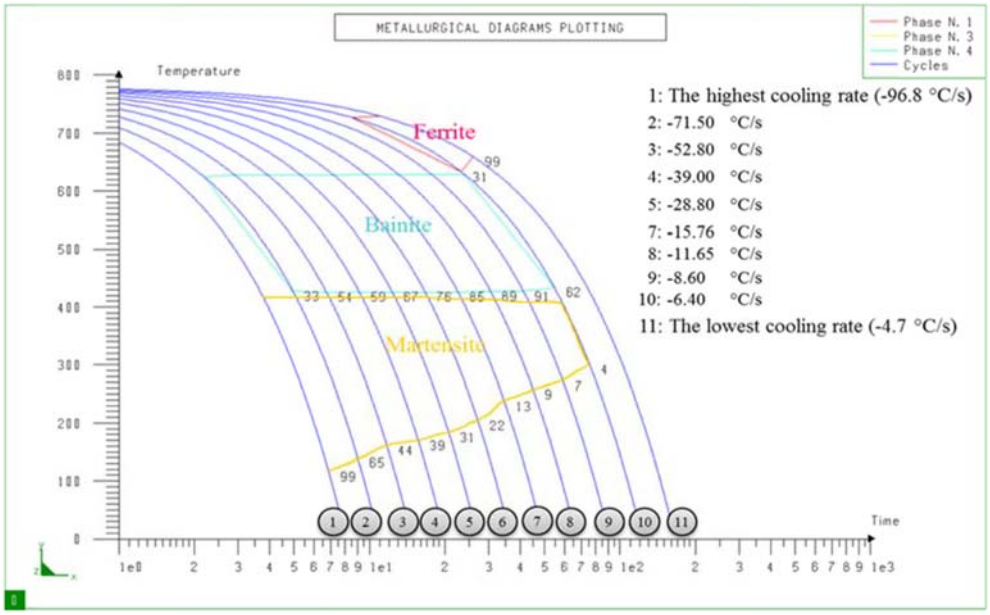

Figure 11. Metallurgical phase diagrams for S355 (SYSWELD® 2013).

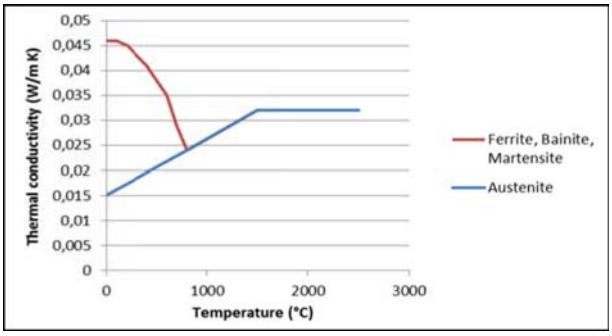

Figure 12. Effect of heat treatment on thermal conductivity (SYSWELD®, 2013).

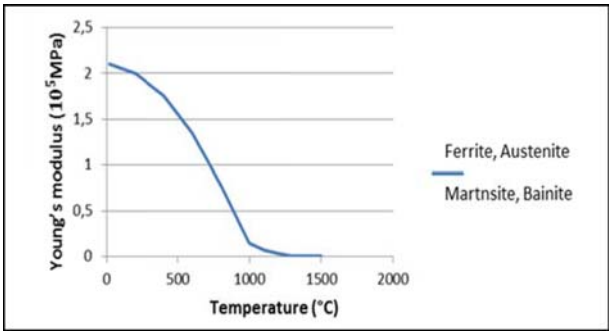

Figure 15. Temperature dependent Young's modulus of (SYSWELD®, 2013).

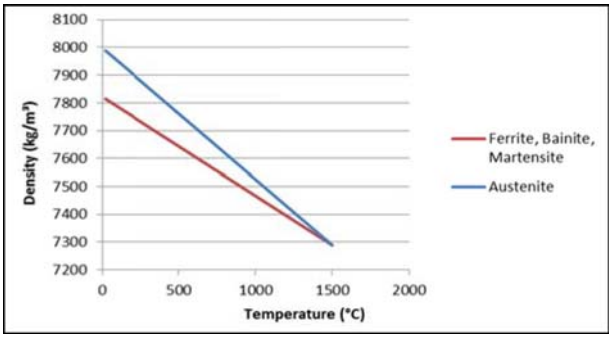

Figure 13. Effect of heat treatment on density (SYSWELD®, 2013).

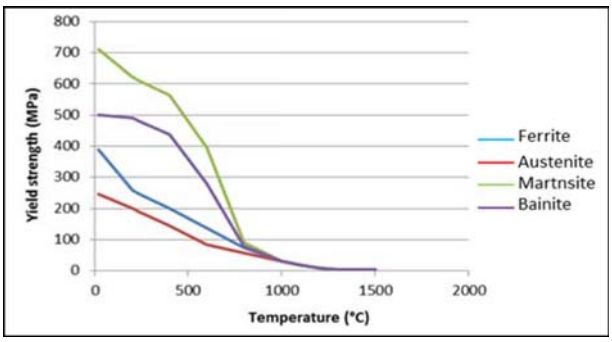

Figure 16. Temperature dependent yield strength in different phases (SYSWELD®, 2013).

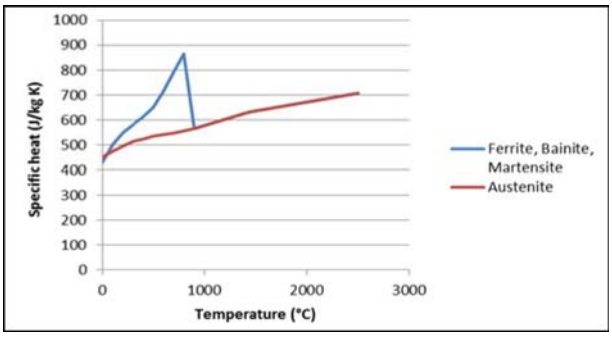

Figure 14. Effect of heat treatment on specific heat per unit of mass (SYSWELD®, 2013).

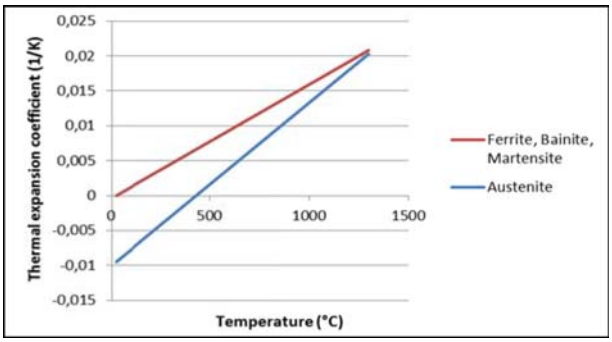

Figure 17. Thermal expansion coefficient for different phases (SYSWELD®, 2013).

Principally when a metal is heated its density decreases. Density is also strongly affected by the quantity of the phase transformation. Typical of this martensite, has a lower density than austenite (Fig. 13), so that the martensitic transformation results in a relative change of volume.

Figure 14 represents the ability of phases to absorb heat from their surroundings. Ferrite, bainite, and martensite experience a variable status with an increase in temperature while austenite possesses a steady state.

According to the Zhou *et al.* (2008) studies, as the mechanical properties of material are temperature dependent, the calculation of temperature field and stress field is defined as non-linear thermal-mechanical couple analysis.

Figure 15 gives the curves of Young's modulus E, yielding stress which changes with time. The temperature dependent yield strength for ferrite, martensite, bainite and austenite are shown in Fig. 16. When steel is subjected to elevated temperatures numerous different solid state reactions can take place. These lead to the formation of different precipitates resulting in detrimental changes in the properties of the material, especially in its toughness (Topolska and Labanowski, 2009). During heat treatments in high temperature steel materials are prone to microstructure changes and precipitation of intermetallic phases. These precipitates are very harmful for the mechanical properties and corrosion resistance of the steel.

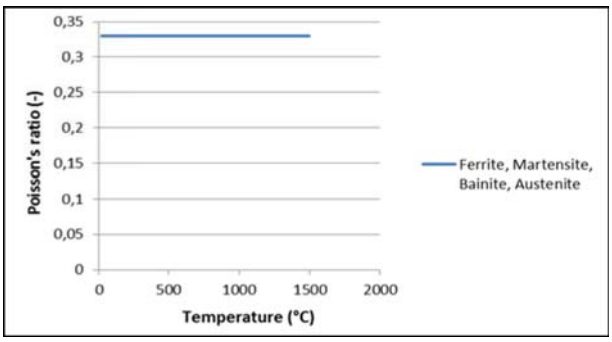

Figure 18. Relationship between Poisson's ratio and temperature (SYSWELD®, 2013).

The coefficient of thermal expansion results as observed in Fig. 17 were expressed as dimension change as a function of temperature. It is observed that the rate of dimension change versus temperature for austenite becomes more.

It was also discovered that Poisson's ratio are taken constant and predicted a value ν=0.33 as shown in Fig. 18.

Including above figures there has been found by Zhu and Chao (2002) to investigate the effects of temperature-dependent material properties on transient temperature. The yield stress is the key mechanical property in welding simulation. Its value has significant effect on the residual stress and distortion. Armentani *et al*. (2007) analyzed, a non-uniform temperature distribution is a main concerning during the welding. This distribution initially causes a rapid thermal expansion followed by a thermal contraction in the weld and surrounding areas, thus generating inhomogeneous plastic deformation and residual stresses in the weldment when it is cooled. As it is well known, the residual stresses have a strong influence on weld deformation, fatigue strength, and fracture toughness. Thus, it is important to evaluate the residual stresses due to welding. In fact thermal and mechanical properties of materials depend on temperature. Figure 19 represents stress-strain curves for various temperatures.

As it has been exhibited in this figure the stress-strain curves were separated for different temperature in any phase. At small plastic strains around 0.07 the low temperature hardening is high. Equally the martensite suggests high hardening behavior in comparison with other phases. Wittwer and Enzinger (2011) have mentioned that in order to mimic the heat input during the stud welding process, the three dimensional Goldak heat source turned out to be the best way to model the heat input.

$$q=q_0\, e^{-3\left(\frac{x}{x_0}\right)^2} e^{-3\left(\frac{y}{y_0}\right)^2} e^{-3\left(\frac{z}{z_0}\right)^2} \tag{1}$$

$$q_0=\eta\frac{6\sqrt{3}}{\pi\sqrt{\pi}}\frac{UIf}{z_0 y_0 x_0^2} \tag{2}$$

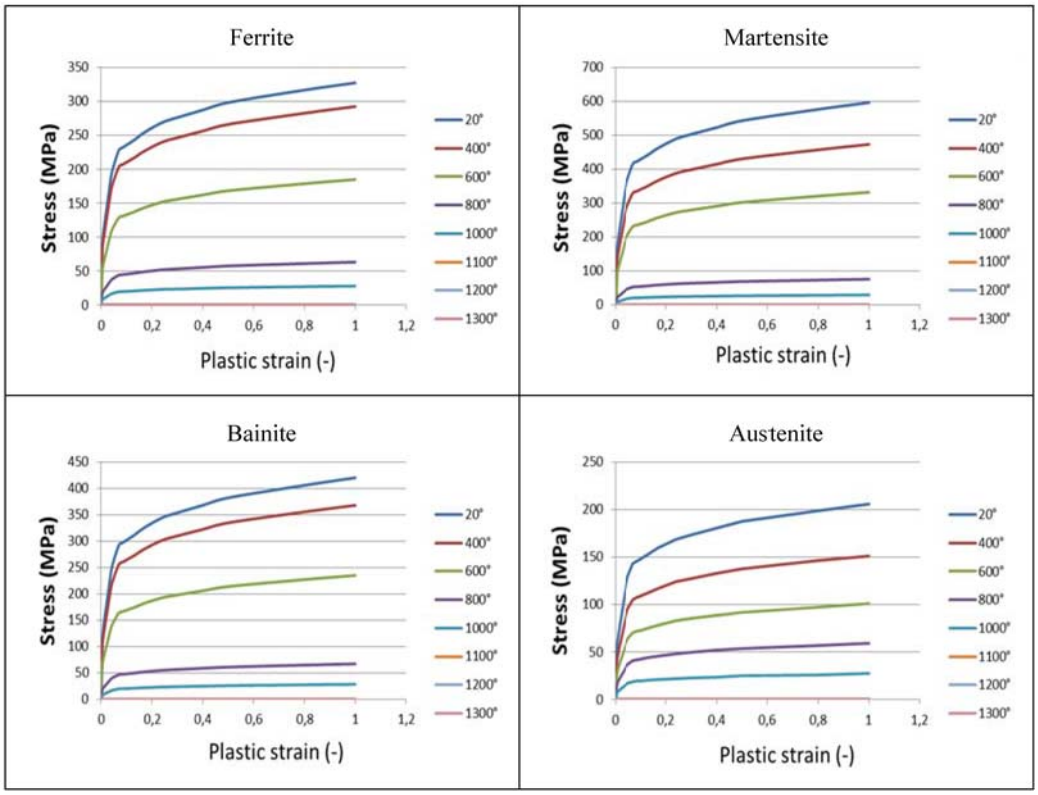

Figure 19. Stress-strain curves for various temperatures (SYSWELD®, 2013).

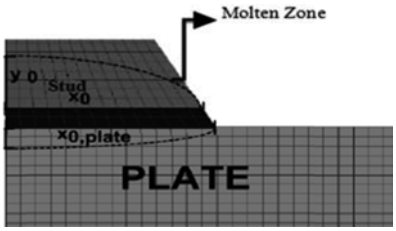

Figure 20. The region of the stud-plate interface (Wittwer and Enzinger, 2011).

X_0, Y_0, and Z_0 (Fig. 20) represent the width, the depth and outer surface dimension of the weld pool, respectively. The parameters U and I are the voltage and electric current defining in connection with the efficiency η the power input. The heat source was split into two parts, one acting on the plate and the other acting on the stud. The parameter f in Eq. (2) describes how much power is deposited on the stud and the plate, respectively. Thus the value of f ranges from 0 to 1 in the stud and the plate and the sum of f_{stud} and f_{plate} must be equal to one due to energy conservation:

$$f=f_{stud}+f_{plate}=1 \tag{3}$$

It has been founded that (GSI SLV München, 2011) stress transfer occurs through a thermal changing. The nonlinear thermal treatment due to the high temperatures introduced during welding and subsequent cooling of the welded metal residual stresses and distortions can be produced. Hence the thermal effect from arc welding and heat treatment influence the microstructure and mechanical properties of welds. In addition to this, residual stresses are as interaction between mechanical, thermal and metallurgical process due to inhomogeneous temperature fields and phase distribution. Figures 21and 22 show the global geometry of stud welding and thermal transient at different times (0.350 s, 1 s, 3 s, 10 s) for 235 MPa steel of stud (0.139%C, 0.225%Si, 0.526%Mn, 0.048%Cr, 0.012%Ni, 0.0%Mo) of 12 mm thickness while 355 MPa has been considered for parent metal plate of 10 mm thickness (0.162%C, 0.282%Si, 1.508%Mn, 0.013%Cr, 0.013%Ni, 0.005%Mo). With respect to the GSI SLV München arc voltage-U=30 V, welding current-I=1050 A and welding time-t=0.35 s were deposited. Volumetric changing is induced when solid phase transformations from austenite to ferrite, bainite, martensite take place during cooling. Cho and Kim (2002) explain that if a significant martensite volume increase take place due to rapid cooling, resulting high compressive stresses can occur in the vicinity of the weld center.

The welding residual stress has great influence on the design of stud welding structure and of the strength. In practical usage, the accumulating residual stress might exceed the practical bearing capacity of the studs on the condition of designing loads. Thus, the stud welded could

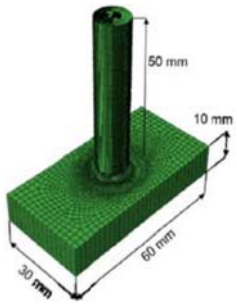

Figure 21. Global geometry of stud welding (GSI SLV München, 2011).

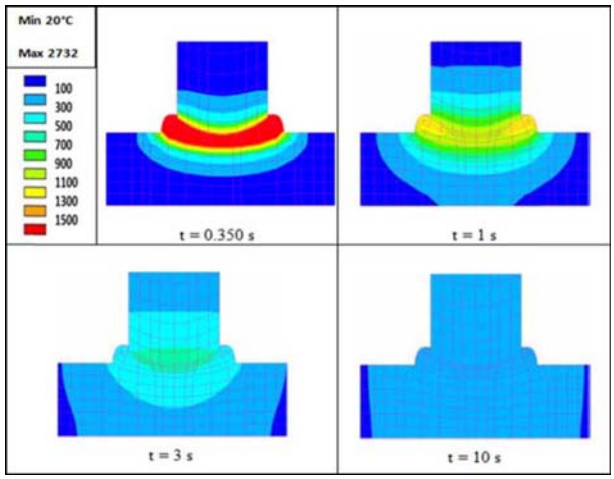

Figure 22. The thermal transient in 0.350s, 1s, 3s, 10s (GSI SLV München, 2011).

rupture when the load is lower than the designing load (Zhou *et al*., 2008). This section addresses the residual stress of related works which have been incorporated into discussions in various fields. Feng (2005) described that the complicated heat and mass transfer and fluid flow phenomena in welding can result in the formation of residual stresses in the joint region and distortion of the welded structure. Wang *et al*. (2011) stated that in the stud welding operations metals are heated up to the melting state during an electrode flows due to electrical resistance. After finishing the joining operation, owing to the non-uniform temperature distribution, residual stresses are introduced within the metal where they have self-equilibrium state.

5.1. Temperature consideration for stresses

The majority of the mechanical properties are based on the chemical composition of steels because it indicates the required heat treatment data, i.e. phase transformation temperatures and critical cooling rate (Htun *et al*., 2008). Lambers *et al*. (2011) mentioned that phase transformations have to be considered since they are accompanied by volumetric changes which might be lead to distortion. Thus, for the optimization of the temperature-time-deformation

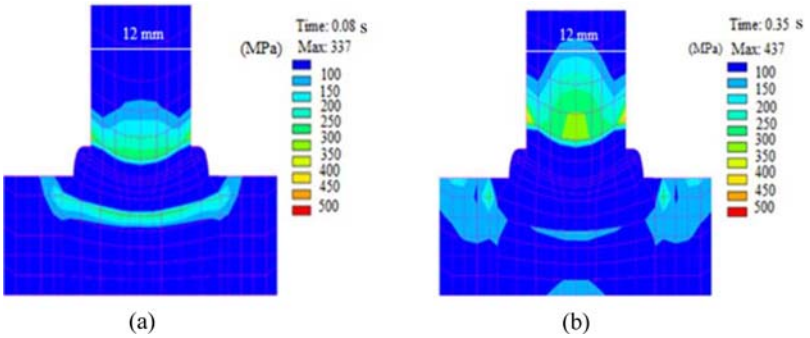

Figure 23(a). Stress state at 0.08s for Steel 235 with M12 stud (during the welding process) (GSI SLV München, 2011).
Figure 23(b). Stress state at 0.35s (end of welding time) for Steel 235 with M12 stud (GSI SLV München, 2011).

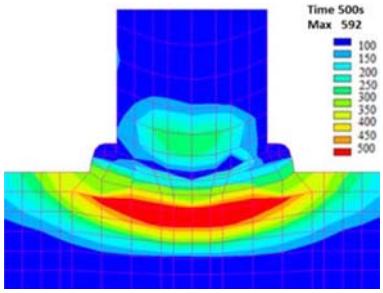

Figure 24. Stress state at 500s (end of the welding process) (GSI SLV München, 2011).

it is indispensable how the different parameters, such as temperature affect the phase transformation behavior and the mechanical properties. Mebaraki *et al*. (2002) studied that mechanical properties and particularly yield stress of steels for high temperature are strongly influenced by heat treatments. A compressive stress field is formed near the high temperature region, whereas a tensile stress is formed in the relatively low temperature region (Rocha *et al*., 2012). As Sluzalec (2005) debated stresses within a short distance from the heat source are compressive, because the expansion of these areas is restrained by the surrounding metal where the temperatures are lower. Since the temperatures of these areas are high and the yield strength of the material low, stresses in these areas are as high as the yield strength of the material at corresponding temperatures. As time progresses, as shown in Fig. 23, the temperatures in the hot weld center line region decrease, whereas temperatures in the surrounding cold region start to increase due to heat conduction from the fusion zone (Rocha *et al*., 2012). Woo *et al*. (2011) concluded that excessive residual stresses are known to degrade the structural integrity and performance of components. Figure 24 demonstrates the stress state within cooling process and after reaching to room temperature by dissipating the thermal energy into air.

Since most matching data are achieved with the proper established model, the welding simulation is an accepted means for determining the structure, default and residual stresses in welded components (GSI SLV München, 2011). Tensile strength quality is one of the key factors in achieving good welding process performance. The tensile strength of stud welding process is mostly affected by welding time factor (Fig. 25), followed by sheet coating factor and stud material factor (Hamza, 2012).

6. Weld Fatigue Life

Fatigue cracking during service is a major concern for ongoing structural integrity of welds. Fatigue failures usually

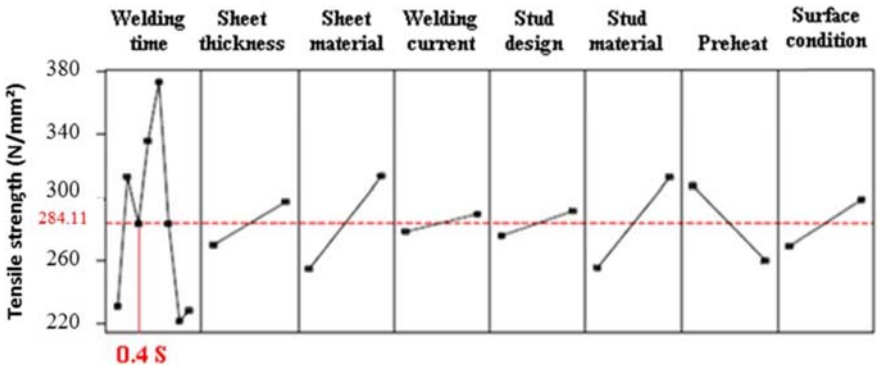

Figure 25. Main effects plot for the mean response of stud arc welding (Hamza, 2012).

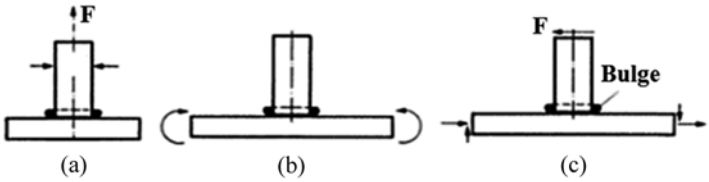

Figure 26. Stud welded joints, subjected to loading by running-through tension (a), base plate bending (b), and stud transverse force (c) (Radaj, 1990).

initiate at changes in cross section and sharp flaws or at welds. The sharper the notch, the higher the stress concentration: and the greater the limitation on fatigue life. A poorly shaped weld cap with a sharp transition between the weld and the parent metal will also have an adverse effect on fatigue performance (Moore, 2009). In the presence of time variable, frequently repeated (cyclic) loading, plastic deformation occurs at the microscopic and macroscopic level, which decreases future ability to withstand stress and initiates cracks. At low temperatures the fatigue strength of materials increases in a similar manner to the static strength and it decreases at high temperatures (Radaj, 1990).

In general, Kirkhope *et al*. (1999) divided weld fatigue improvement methods into two main groups; Weld geometry modification methods and residual stress methods. The weld geometry modification method is one of the techniques which relies on mechanical means to improve the weld profile thus reducing the weld stress concentration. Earlier investigations on welded studs showed decreased fatigue strength of the parent metal due to the notch effect of the weld. The fatigue strength decreased with increasing stud diameter, but recovered by post-heating (Fricke and Tchuindjang, 2012). Fatigue cracks initiate, as shown in Fig. 26, at the sharp notch under the bulge and propagate in the stud if stud tension runs straight through (a) (rare in practice). If there is tension or bending in the base plate (b) (including stud transverse force (c)) they propagate in the base plate, approximately normal to the principle loading direction, adjacent to the stud weld base at the front face (Radaj, 1990).

Idris and Prawoto (2012) inferred that the fatigue crack propagation rate was influenced by the ferrite content. This indicates that a ductile material has a lower fatigue crack growth rate than the brittle material. In other words, when the ferrite fraction is higher, the higher ductility drives the fatigue life up. The strength increases and ductility decreases with increasing martensite volume fraction (MVF). Most of the fatigue cracks were initiated at the martensite-ferrite interfaces as shown in Figure 8 before and ferrite grain boundaries when the ferrite fraction is higher. The arrangement of the microstructure is roughly proportional to the temperature at which the specimens were heated. The interrelated experimental results by Lin and Perng (1997) have shown that the residual stress is increased with the heat input during welding. Using a higher welding heat input increased the amount of heat going into the weldment and elevated the martensite phase transformation temperature. Residual stresses could not be significantly reduced by increasing preheat (interpass) temperature while welding. Using higher preheat temperature conditions could elevate the equilibrium temperature and the martensite phase transformation temperature and increased the heat input to the weldment. Guo (2012) mentioned materials with lower austenite stability generally show higher susceptibility to delayed fracture. It was found by Han *et al*. (2012) that with the increase in quenching temperature, the strength increases, while the elongation and toughness decrease. Microstructural examination revealed that the laths of martensite and bainite become coarser with the increase of either quenching or tempering temperature. Yu-ichi (2007) revealed the fatigue crack growth rate was decreased drastically when the crack proceeded to the surface of the bainite layer from the ferrite layer. Kudryavtsev and Kleiman (2001) suggested that improvement in the fatigue strength of the welded joint could be obtained if tensile residual stresses were removed. However, a greater benefit can be realized if compressive residual stresses are introduced at the weld region. Equally it has been mentioned that by Chobaut *et al*. (2012) fast quenching is desired to avoid coarse precipitation, which reduces the mechanical properties. However this leads to high residual stresses, which case unacceptable distortions and reduce service life drastically.

7. Evaluation Method

The American National Standard Institute (1993) recommended practices and the variations of the process for stud welding. Nevertheless, all physical and chemical properties are independent of stud size or shape.

7.1. Base metal

7.1.1. Low carbon steel

Low carbon steels, as used for fasteners, are defined as those with insufficient carbon content to permit a predictable response to a strengthening heat treatment process. The low carbon steel fastener according to the ASTM A307 is a special bolt used in piping and flange work. Low carbon (mild) steels can be stud welded with no major metallurgical problems. Low carbon steel physical properties are typically $55*10^3$ psi minimum ultimate and $50*10^3$ psi minimum yield. Nelson studs can be annealed to a maximum 75 Rockwell hardness (HRB) for low carbon

Table 5. Low carbon chemical composition (Nelson Stud Welding, 2013)

Element	Minimum wt%	Maximum wt%
C	0.08	0.23
Mn	0.30	0.90
P	-	0.04
S	-	0.05

steel. The following table (Table 5) expresses the low carbon steel chemical composition (Nelson Stud welding, 2013).

7.1.2. Medium and high carbon steel

Medium carbon steels are heat treatable, which means that through metallurgical treatments the tensile strength of the fastener after processing can be significantly higher than that of its original raw material. The range of carbon content in this steel is from 0.25 to 0.70% (The Bolt supply House Ltd., 2013). In contrast, the range of carbon from 0.70 to 1.05% is classed for high carbon steels (Seblin *et al*., 2014). It will withstand high shear and will thus be subjected to little deformation. If medium and high-carbon steel are to be stud welded, it is imperative that preheat be used to prevent cracking in the heat-affected zones. In some instances, a combination of preheating and post heating after welding is recommended. In the case of tough alloy steels, either preheating or post heating may be used to obtain satisfactory results. As Ismar *et al.* (2012) cited for high-strength steels weldments have to be achieve equal strength. High residual stress in those welds diminishes the components safety.

7.1.3. Low alloy steel

Generally, the high strength, low alloy steels are satisfactory stud welded when their carbon content is 0.15 percent or lower. If carbon content exceeds 0.15 percent, it may be necessary to preheat the work to a low preheat temperature to obtain desired toughness in the weld area. When the hardness of the heat-affected zones and the stud fillet does not exceed 30 Rockwell C, studs can be expected to perform well under almost any type of serve service. According to Chambers (2001) investigations all too often stud and base plate materials must be compatible with the stud welding process. Commonly used studs in the precast and construction industries are governed by the following American Welding Society (AWS, 2013) codes (Table 6):

7.2. Fatigue assessment

Based on forenamed reasons, the objectives of this part are the following:

- To describe and present the test procedures
- To discuss the applicable S-N curves

Based on Offshore Technology Report (2002) retrieved from Eurocode 3, S-N curves are referred to as "fatigue strength curves" and partial safety factors are applied to these according to accessibility of the component during periodic inspection and maintenance, and the consequence of failure.

- To evaluate the factors influencing the fatigue life
- To generalize methodology for research on fatigue behavior

The fatigue failure of the shear stud connection is defined as the failure of the steel detail itself (Odenbereit *et al*., 2004). Based on research report (Xie, 2011),

Table 6. Minimum mechanical property requirements for studs (Chambers, 2001)

Property	Type A (AWS)	Type B (AWS)	Type C (ASTM A 496)
Tensile strength	61000 psi (420 MPa)	65000 psi (450 MPa)	80000 psi (552 MPa)
Yield strength (0.2 % offset)	49000 psi (340 MPa)	51000 psi (350 MPa)	Not specified
Elongation (Percent in 2 in.)	17	20	Not specified
Percent area reduction	50%	50%	Not specified

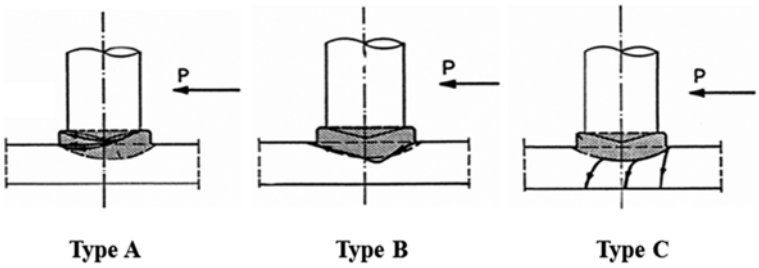

Figure 27. Failure models of Shear studs under fatigue loading (Xie, 2011).

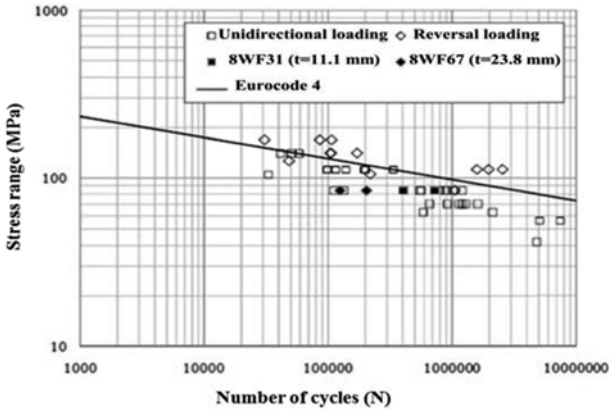

Figure 28. S-N curves for stud test results by Slutter and Fisher (Xie, 2011).

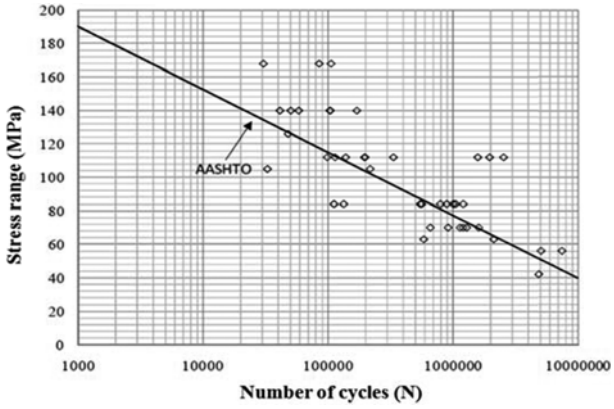

Figure 29. Comparison of test results and the provision of AASHTO (Xie, 2011).

Hallam (1976) summarized three types of fatigue cracks as depicted in Fig. 27.

In Type A, the beginning of crack formed at the stud shank and the successive crack forms through the shank and the weld collar respectively; in Type B the beginning of crack formed at the foot of the weld collar and courses the region of welding influence in the flange material. In the Type C, the beginnings of crack formed at the foot of the weld collar and successive crack forms either directly through the flange or first alongside the welding influence zone and then through the flange.

Regarding the factor influencing the fatigue life, several most important ideas have been turned out for fatigue behaviors of headed studs.

(1) The stress range instead of peak load is the main influencing factor for the fatigue life and the relationship between the stress range and fatigue life could be explained as a line in double logarithm diagram.

(2) Under the same stress loading ranges, the test result indicated that the studs under unidirectional loading had a lower fatigue life than under reversal loadings.

(3) Flange thickness of the steel beam also affects the fatigue life of headed studs, the thicker the flange is, the lower fatigue it would be.

In this study the fatigue strength design criterions for shear studs were described in two international codes including Eurocode 4 and American Association of State Highway and Transportation Official (AASHTO) (Trillmich and Welz, 1997).

A fatigue strength curve (Fig. 28) -the so called Wöhler curve- to determine the lifetime for shear studs from Eurocode 4 was derived. This equation is:

$$\text{Log } N+8 \text{ log } \Delta\tau=21.93 \quad (4)$$

Although compared to Eurocode 4 nowadays, these tests results got nearly 50 years ago are much lower, because of the poor weld technology that time, the fatigue features are clear.

The equation in AASHTO transformed to relationship

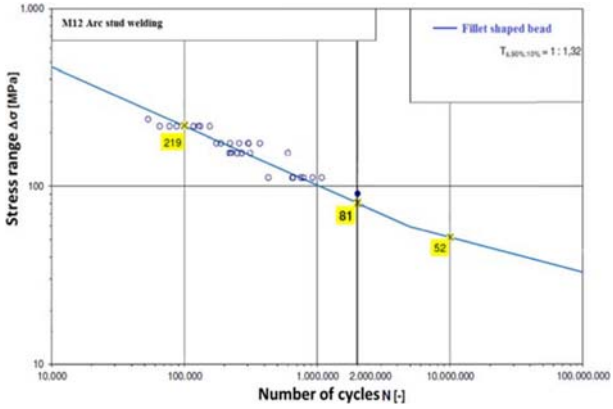

Figure 30. S-N curves diagram according to Euro Code 3/3 at $2*10^6$ load cycles (GSI SLV München, 2011).

of stress range and fatigue life is:

$$\Delta\tau=\frac{4}{\pi}(238\text{-}29.51 \text{ log } N) \quad (5)$$

Which they could be explained as a line in double logarithm diagram as plotted in Fig. 29.

From these two tests, it can be debated some important ideas for fatigue behaviors of headed studs.

• The stress range instead of peak load is the main influencing factor for the fatigue life.

• Under the same stress loading ranges, the test result indicated that the studs under unidirectional loadings had a lower fatigue life than under reversal loadings. Accordingly to the SLV München investigation (Fig. 30), based on the fracture specimens at $2*10^6$ load cycles for each test series, a Wöhler curve has been determined according to Euro code to specify the fatigue strength. The mean fatigue strength $\Delta\sigma$ at $2*10^6$ load cycles the amount of 81 MPa for the ceramic ferrule stud welding has been found.

7.3. Remarks

From the results of fatigue effects, it can be observed that the various factors that influence the fatigue life are:

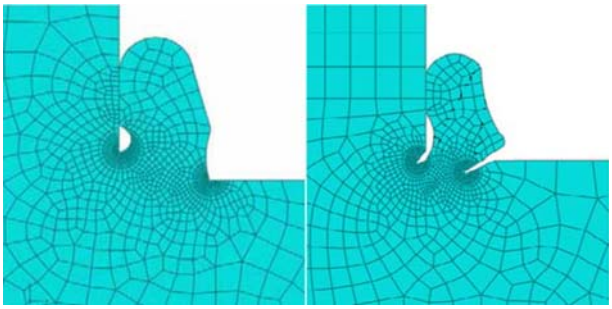

Figure 31. Notch effect with different size and shape (GSI SLV München, 2011).

• Material properties

Material properties affect the fatigue resistance in various ways and the most important properties are described here. Sherman and Davies (1981) obtained that carbon content of the phases also appears to play a role, particularly for cyclic properties. At constant martensite contents higher carbon levels result in better fatigue properties.

• Effect of static strength

The ultimate strength of material has less influence on the fatigue, for high strength materials this effect is stronger than for ordinary materials. High elongation steels are more beneficial in the region of short fatigue life, while high tensile strength steels have more advantages in the long life region (Kwon and Chung, 2011). It was deduced by Fleck and Smith (1981) the yield stress and ultimate tensile stress resistance to fatigue crack propagation.

• Crack growth data

The crack growth is less dependent on static strength than crack initiation. Sudhakar and Dwarakadasa (2000) observed that fatigue crack growth rate decreases with an increase in martensite content. As Johnson (2000) investigated, for a fatigue load varying between a maximum value, σ_{max}, and minimum value, σ_{min}, the stress intensity factor varies between K_{max} and K_{min} and thus over a range $\Delta K = K_{max} - K_{min}$. For members where cracks are initiated during the fatigue loading, there exists a fatigue-crack propagation threshold. Below this threshold-value existing fatigue cracks will not propagate. When K is above the threshold value, cracks will propagate due to the fatigue loading, and eventually cause the fracture of the structure.

• Notch effect

Notch is discontinuity in the material that comes from welds or holes for studs (Fig. 31). Notch can also come from mechanical influence. Fatigue life is affected if the part is notched; the notch is acting like an initiation of a crack. According to Yen and Dolan (2007) investigation for ductile metals the presence of a notch usually reduces the fatigue strength. It is generally believed that hard steels are more notch-sensitive than soft steels. Pure metals and very fine-grained metals appeared most sensitive to the effect of notches. The more severe the notch, the less is the percentage gain in fatigue strength. In this regards, Hensel *et al*. (2012) declared that cracks not only release initial residual stresses but generate new tensile residual stresses in the surrounding of a crack.

• Size effect

Increasing the size of a structure generally gives a lower resistance to fatigue. This means that the specimens tested in laboratory will possess a higher resistance than the structure in use, since the test specimens are as small as possible.

• Residual Stress effect

Residual stresses may affect the fatigue life in both increase or decrease fatigue of the life. Increase of fatigue life appears when the residual stresses have opposite direction than the stress that is causing the crack propagation. If the residual stress has the same direction as the stress that cause the crack propagation the fatigue life is reduced.

The bearing capacity of welded studs should be basically equivalent bearing capacity of unwelded studs. An even, fully closed weld collar with a shiny surface and a sufficient quantity of material melt from the stud (the nominal length of the stud is reached only after welding) are considered as signs of satisfactory welding quality. In other words a weld collar of uneven height indicates a blowing effect which can be avoided or at least reduced by appropriate measures (Trillmich and Welz, 1997). Above all, it has been related by Zhu *et al*. (2012) in the high cycle fatigue regime, the influence of microstructures on fatigue performance was greater than that of micro defects.

The investigations have been shown by Loukus *et al* (2004) that the existence of a weld; its geometry and its microstructure determine the failure characteristics. Microstructural observations revealed that the weld regions are less ductile than the no-weld regions. The rate of quenching is carefully controlled to retain a fine dispersion of vacancies, which leads to enhancement of mechanical properties of the material in the subsequent stages of heat treatment. The UTS and yield strength are moderately affected by the weld but a greater reduction in ductility of the material is noticed when the weld material volume is greatly increased in the specimens.

8. Conclusion

Current research focused on prediction of stud welding process behavior, stud diameter effects, and influence of the material strength and hardening behavior as well as metallurgical effects on fatigue strength. After reviewing by numerous investigations it appears that fatigue strength of metal member depends on different factors. Chiefly; energy input, thermal and mechanical behavior as well as their interactions during welding process and metallurgical hardening.

It has been found by Htun *et al*. (2008), the fatigue properties were affected by phase changes. Typical of this, a small amount of ferrite appears to improve the

fatigue strength. It also mentioned by Yen and Dolan (2007) that metals with inherent defects such as notch and tensile residual stresses develop localized stresses that may serve to initiate a fatigue crack. Similarly since the yield tensile stresses are commonly encountered in welded components, consequently these may reduce fatigue life or increase susceptibility to failure mechanisms (Dai *et al*., 2008). In collaboration with results it has been debated that stresses are concentrated in the stud and in the HAZ. Beside that lower HAZ hardness and smaller HAZ size improve tensile impact.

It has been tried to be expressed the important and effective parameters including:

1. Available processes for stud welding
2. How strong the joint can be since the stud is joined with the workpiece over the whole surface.

Moreover for future investigation using the variety fields described (electric field, temperature field, and mechanical filed); the effect of fatigue strength for stud welding can then be simulated for the purpose of analysis accordingly and consequently the simulation of the stud welding offers an opportunity to gain insight into the thermo-metallurgical and mechanical process during the joining process.

References

Al-Sahib, N. K. A., Ameer, H. K. A., and Ibrahim, S. G. F. (2009). "Monitoring and quality control of stud welding." *Al-Khwarizmi Engineering Journal*, 5(1), pp. 53-70.

Ambriz, R. R. and Mayagoitia, V. (2011). *Welding of Aluminum alloys, recent trends in processing and degradation of Aluminum alloys*. InTech.

American National Standards Institute (1993). *Recommended Practices for stud welding*. AWS committee on Arc Welding and Cutting, American National Standards Institute.

Armentani, E., Esposito, R., and Sepe, R. (2007). "The effect of thermal properties and weld efficiency on residual stress in welding." *Journal of achievements in Materials and Manufacturing Engineering*, 20, pp. 319-322.

AWS (2013). Welding Time and Current Settings. American Welding Society, Taylor Company, Available in: <http://www.taylor-studwelding.com>, retrieved April 15, 2014.

Behrens, B. A. Gruß, D., and Jenicek, A. (2011). "Stud welding within sheet metal working tools." *Proc. Eng. Res. Devel*., Vol. 5, pp. 283-292.

Bhadeshia, H. K. D. H. and Honeycombe, R. (2006). *Steels microstructure and properties. 3rd edition*., Elsevier Ltd.

The Bolt supply House Ltd. (2013) Technical *catalogue of materials-carbon and alloy steels.* Available in: <http://www.boltsupply.com/catalogue_files/catalog_data/toc_data/pdf/007.pdf>, retrieved April 15, 2014.

Calcagnotto, M. Adachi, Y. Ponge, D., Raabe, D. (2011). "Deformation and fracture mechanisms in fine-and ultrafine-grained ferrite/martensite dual-phase and the effect of aging." *Acta Materialia*, 59, pp. 658-670.

Chambers, H. A. (2001). "Principles and practices of stud welding." *PCI Journal*, pp. 45-58.

Cho, S. H. and Kim, J. W. (2002). "Analysis of residual stress in carbon steel weldment incorporating phase transformations." *Science and Technology of Welding and Joining*, 7, pp. 212-216.

Chobaut, N., Repper, J., Pirling, T., Carron, D., and Drezet, J. M. (2012). "Residual stress analysis in AA7449 As-quenched thick plates using netrons and FE modeling." *Proc. 13th International Conference on Aluminum Alloys (ICAA13)*, Canada, pp 285-291.

Clegg, M. A., Cook, R. C., and Fraser, R. W. (1983). *A new method of wear resistant surfacing by welding*. DVS-Berichte, Schweisstechnische Beschichtungsverfahren, pp. 16-20.

Dai, H. (2012). Modelling residual stress and phase transformations in steel welds. InTech.

Dai, H., Francis, J. A., Stone, H. J., Bhadeshia, H. K. D. H., and Withers, P. J. (2008). "Characterizing phase transformations and their effects on ferritic weld residual stresses with X-rays and Neutrons." *Metallurgical and Materials Transactions*, 39, pp. 3070-3078.

David, S. A. Babu, S. S., and Vitek, J. M. (2003). "Welding; Solidification and Microstructure." *JOM*, 55, pp. 14-20.

Dean, D., Shoichi, K., Hisashi, S., Hidekazu, M., and Yukihiko,H. (2007). "Numerical investigation on welding residual stress in 2.25 Cr-1Mo steel pipes." *Transactions of JWRI*, 36, pp. 73-90.

Dong, P., Li, H., and Sun, D. (2013). "Effect of welding speed on the microstructure and hardness in friction stir welding joints of 6005A-T6 aluminum alloy." Materials and Design, 45, pp. 524-531.

Elmer, J. W., Olson, D. L., and Matlock, D. K. (1982). "The thermal expansion characteristics of stainless steel weld metal." *Welding Research Supplement*, pp. 293-301.

Eyres, D. J. and Bruce, G. J. (2012). *Ship Construction*. Butterworth-Heinemann, pp. 81-101.

Feng, Z. (2005). *Processes and mechanism of welding residual stress and distortion*. Woodhead publishing Ltd.

Fleck, N. A. and Smith, R. A. (1981). "Effect of density on tensile strength, fracture toughness, and fatigue crack propagation behavior of sintered steel." *Poweder Metallurgy*, 3, pp. 121-125.

Fricke, W. and Tchuindjang, D. D. (2012). *Fatigue strength behavior of stud-arc welded joints in load-carrying ship structures.* International Institute of Welding.

Gruß, D. (2013) *Bolzenschweißen in Blechumformwerkzeugen, Arc Stud Welding with tip ignition in sheet metal working tools*. Phoenix Feinbau GmbH.

GSI SLV München (2011). *Bewertung und optimierung der tragfähigkeit von gewindebolzenschweißenverbindungen unter ermüdungsbeanspruchung*. Report in SLV München.

Guo, X. (2012). *Influence of microstructure, alloying element and forming parameters on delayed fracture in TRIP/TWIP-aided austenitic steels*. RWTH Aachen University, DE.

Hamza, R. M. A. (2012). *Optimized stud arc welding process control factors by Taguchi experimental design technique*. Gulf University, Kingdom of Bahrain, Chapter 15, pp. 369-394.

Han, Y., Fan, Z., Hao, Y., and Jin-Bo, Q. (2012). "Effect of

heat treatment on the microstructure and mechanical properties of an offshore structure steel E550." *Proc. Asia Steel International Conference*, Beijing.

Hensel, J., Nitschke-Pagel, T., Schönborn, S., and Dilger, K. (2012). "Factors affecting the knee point position of S-N curves of welds with longitudinal stiffeners." *Proc. International Offshore and Polar Engineering Conference*, Greece, pp. 187-192.

Hsu, C. and Mumaw, J. (2011). "Wedability of advanced high-strength steel drawn arc stud welding." *Welding Journal*, pp. 45-53.

Hsu, C., Phillips, D., Champney, C., and Mumaw, J. (2007). *Portable and intelligent stud welding inverter for automotive and sheet metal fabrication*. Robotic welding, Intelligence and Automation, Lecture Notes in Control and Information Science, Vol. 362, pp. 367-374.

Htun, M. S., Kyaw, S. T., and Lwin, K. T. (2008). "Effect of heat treatment on microstructures and mechanical properties of spring steel." *Journal of Metals, Materials and Minerals*, 18, pp. 191-197.

Idris, R. and Prawoto, Y. (2012). "Influence of ferrite fraction within martensite matrix on fatigue crack propagation: An experimental verification with dual phase steel." *Material Science and Engineering*, 552, pp. 547-554.

International Welding Technologies Inc. (2003). *Stud welding technological guide for weld pins.* International Welding Technologies Inc.

Ismar, H., Burzic, Z., Kapor, N., and Kokelj, T. (2012). "Experimental investigation of high-strength Structural steel welds." Journal of Mechanical Engineering, 58, pp 422-428.

Jenicek, A., Bschorr, T., and Cramer, H. (2006). Stud welding on coated sheets in composition. Schweißtechnische Lehr- und Versuchsanstalt (SLV) München, pp 177-182 (in German).

Joarder, A., Saha, S. C., and Ghose, A. K. (1991). "Study of submerged Arc welded metal and Heat-Affected Zone microstructures of a plain Carbon Steel." *Welding Research Supplement,* pp. 141-149.

Johnson, R. P. (2000). "Resistance of stud shear connectors to fatigue." *Journal of Constructional Steel Research*, 56, pp. 101-116.

Khan, M. I., Kuntz, M. L., Biro, E., and Zhou, Y. (2008). "Microstructure and Mechanical Properties of resistance Spot welded Advanced High Strength Steels." *Materials Transactions*, 49(7), pp. 1629-1637.

Kirkhope, K. J., Bell, R., Caron, L., Basu, R. I., and Ma, K.-T. (1999). "Weld detail fatigue life improvement technique. Part 1: review." *Marine structures*, 12, pp. 447-474.

Kitani, Y., Ikeda, R., Yasuda, K., Oi, K., and Ichimiya, K. (2007). "Improvement of HAZ toughness for high heat input welding by using Boron Diffusion from weld metal." *Welding in the World*, 51, pp. 31-36.

Kwon, H. and Chung, Y. (2011). "Influence of tempering temperature on fatigue and mechanical properties of high strength steel." *Proc. International Automotive Body Congress*, Munich, Germany, Available in: <http://bodyandassembly.com/wp-content/uploads/2012/01/Edited-Kwon-Paper.pdf>, retrieved April 15, 2014.

KÖCO (2013). Stud welding-technology. KÖSTER & CO., Available in: <www.bolzenschweisstechnik.de>, retrieved April 15, 2014.

Kudryavtsev, Y. and Kleiman, J. (2001). "Fatigue of welded elements: residual stresses and improvement treatments." *Experimental and Applied Mechanics*, 6, pp. 75- 84.

Kuehn, D. E., Jenkins, J. C., Folkening, R. W., and McClellan, R. (1997). *Stud Welding-Chapter 9*. American Welding Society.

Li, D., Tao, J., Meng, Q., and Fang, H. (2003). "Indirect measurement of material thermal and mechanical properties during welding." *J. Mater. Sci. Technol*., 19, pp. 173-175.

Lin, Y. C. And Perng, J. Y. (1997). "Effect of welding parameters on residual stress in type 420 martensite stainless steel." *Science and Technology of Welding and Joining*, 2, pp. 129-132.

Loukus, A. Subhash, G., and Imaninejad, M. (2004). "Mechanical properties and microstructural characterization of extrusion welds in AA6082-T4." *Journal of Materials Science*, 39, pp. 6561-6569.

Mair, P. (2005). *Assessment of EMF (Electromagnetic field) and biological effects in arc welding applications*. Commission XII, International Institute of Welding.

Masubuchi, K., Ozaki, A., and Chiba, J. J. (1978). "Underwater stud welding." *Proc. Ocean Challenge Fourth Annual Combined MTS-IEEE Conf.*, Washington, pp. 125-129.

Merkabi, N., Lamesle, P., Delagnes, D., and Levaillant, C. (2002). "Relationship between microstructure and mechanical properties of A 5% Cr hot work tool steel." *Proc. 6th International Tooling Conference*, France, pp. 737-754.

Moore, P. L. (2009). "The importance of welding quality in ship construction." *Proc. 2nd International Conference on Marine Structures (MARSTRUCT)*, Lisbon, Portugal.

Nishikawa, W. (2003). "The principle and application field of stud welding." *Welding International*, 17, pp. 699-705.

Nelson Stud Welding (2013). General information for stud welding studs. Available in: <http://www.nelsonstud.com/cat-pdf/generalinfo.pdf>, retrieved April 15, 2014.

NS Stud Welding Method (2013). High quality welding method for deformed bars. Available in: <http://www.nssmc.com/en/tech/report/nsc/pdf/n9232.pdf>, retrieved April 15, 2014.

Odenbereit, C. Leffer, A., and Feldmann, M. (2004). "Fatigue behavior of shear studs to transfer dynamic loads between steel-and concrete construction Elements." *Sea Tech Week-Fatigue of Maritime Structures*, pp. 1-9.

Offshore Technology Report (2002). *Comparison of fatigue provisions in codes and standards.* Bomel Limited, Health and Safety Executive (HSE) Books, UK.

Peet, M. J., Hasan, H. S., and Bhadeshia, H. K. D. (2011). "Prediction of thermal conductivity of steel." *International Journal of Heat and Mass Transfer*, 54, pp. 2602-2608.

Radaj, D. (1990). *Design and analysis of fatigue resistant welded structures*. Woodhead publishing Ltd., Abington Hall, UK.

Ramasamy, S. (2000). "Drawn arc stud welding, Crossing over from steel to aluminium." *Welding Journal*, pp. 35-

39.

Roberts, T. M. and Dogan, O. (1998). "Fatigue of welded shear connectors in steel-concrete-steel sandwich beams." *Journal of Constructional Steel Research*, 45, pp. 301-320.

Rocha, J. D., Arrizabalaga, E. M., Quevedo, R. L., and Morfa, C. A. (2012). "Behavior and strength of welded stud shear connections in composite beam." *Rev. Fac. Ing. University Antioquia N.,* 63, pp. 93-104.

Samardzic, I., Kladaric, I., and Klaric, S. (2009). "The influence of welding parameters on weld characteristics in electric arc stud welding." *Metalurgia,* 48, pp 181-185.

Seblin, B., Jahazeeah, Y., Sujeebun, S., Manohar, W., and Ky, B. (2014). *Material science-MECH 2104*. pp. 1-21, Available in: <http://www.uom.ac.mu/faculties/foe/mped/students_corner/notes/enggmaterials/steelbklet.pdf>, retrieved April 15, 2014.

Sherman, A. M. and Davies, R. G. (1981). "Influence of martensite carbon content on the cyclic properties of dual phase steel." *International Journal of Fatigue*, 3, pp. 195-198.

Sluzalec, A. (2005). *Theory of thermo mechanical processes in welding*. Technical university of Czestochowa Poland.

Srivastava, B. K., Tewari, S. P., and Prakash, J. (2010). "A review on effect of arc welding parameters on mechanical behavior of ferrous metals/alloys." *International Journal of Engineering Science and Technology*, 2(5), pp. 1425-1432.

Sudhakar, K. V. and Dwarakadasa, E. S. (2000). "A study on fatigue crack growth in dual phase martensitic steel in air environment." Bulletin of Materials Science, 23, pp. 193-199.

SYSWELD® (2013). *2013 Reference Manual*. ESI Group, Paris.

Tank Car Committee (2013). *Agenda-Background.* Tank Car Committee, Subcommittee 2, Colorado Springs Co., pp. 1-51.

Topolska, S. and Labanowski, J. (2009). "Effect of microstructure on impact toughness of duplex and superduplex stainless steels." *Journal of Achievement in Materials and Manufacturing Engineering,* 36, pp. 142-149.

Trillmich, R. and Welz, W. (1997). *Bolzenschweißen, Grundlagen und Anwendung (Fachbuchreihe Schweißtechnik Band 133). DVS-Verlag*, Düsseldorf, Germany (in German).

Wang, L., Zhang, Q., and Chen, L. (2011). "Residual stress simulation of stud welding in a rectangular steel tubular surface." *Applied Mechanics and Materials*, 44-47, pp. 581-585.

Williams, H. E., Ottsen, H., Lawrence, F. V., and Munse, W. H. (1970). *The effects of weld geometry on the fatigue behavior of welded connections.* Interim report on IHR-64 behavior of welded highway structures, University of Illinois.

Wittwer, L. and Enzinger, N. (2011). *Simulating the welding process of pin structures.* Institute for Material Science and Welding, Graz, pp. 45-54.

Woo, W., Feng, Z., Wang, X.-L., and David, S. A. (2011). "Neutron diffraction measurements of residual stresses in friction stir welding: a review." *Science and Technology of Welding and Joining,* 16, pp. 23-32.

Xie, E. (2011). *Fatigue strength of shear connectors*. Research Report, University of Portugal.

Yen, C. S. and Dolan, T. J. (2007). *A critical review of the criteria for notch-sensitivity in fatigue of metals*. University of Illinois Bulletin, pp. 3-55.

Yu-ichi, K. (2007). "Status and prospects of shipbuilding steel and its weldability." *Transactions of JWRI*, 36, pp. 1-6.

Zhou, G., Liu, X., Liang, G., Liu, P., Yan, D., and Fang, H. (2008). "The simulation of residual stress for stud welding and establishment of strength estimating model." Material Science Forum, 575-578, pp. 816-820.

Zhu, M. L., Xuan, F. Z., and Chen, J. (2012). "Influence of microstructure and microdefects on long-term fatigue behavior of a Cr-Mo-V steel." *Material Science and Engineering*, 546, pp. 90-96.

Zhu, X. K. and Chao, Y. J. (2002). "Effect of temperature-dependent material properties on welding simulation." *Computers and Structures*, 80, pp. 967-976.